Induced moduli oscillation by radiation and space expansion in a higher-dimensional model

Hajime Otsuka[1,*] and Yutaka Sakamura[2,3,†]

[1]*Department of Physics, Kyushu University, 744 Motooka, Nishi-ku, Fukuoka, 819-0395, Japan*
[2]*KEK Theory Center, Institute of Particle and Nuclear Studies, KEK, 1-1 Oho, Tsukuba, Ibaraki 305-0801, Japan*
[3]*Graduate University for Advanced Studies (Sokendai), 1-1 Oho, Tsukuba, Ibaraki 305-0801, Japan*

(Received 9 May 2024; accepted 22 May 2024; published 20 June 2024)

We investigate the cosmological expansion of the 3D space in a 6D model compactified on a sphere, beyond the 4D effective theory analysis. We focus on a case where the initial temperature is higher than the compactification scale. In such a case, the pressure for the compact space affects the moduli dynamics and induces the moduli oscillation even if they are stabilized at the initial time. Under some plausible assumptions, we derive the explicit expressions for the 3D scale factor and the moduli background in terms of analytic functions. Using them, we evaluate the transition times between different cosmological eras as functions of the model parameters and the initial temperature.

DOI: 10.1103/PhysRevD.109.115019

I. INTRODUCTION

The existence of extra dimensions is predicted in string theory. Since the experimental constraints on the size of the extra dimensions that the gravity feels are much weaker than those for the standard model particles, there is a wide allowed parameter space for braneworld models with relatively large extra dimensions [1–3]. These types of models have been considered not only as a solution to the large hierarchy problem, but also as a solution to the cosmological constant problem [4]. Recently, it is also pointed out that a micron-size large extra dimension may be predicted by the swampland conjecture [5], which is called the dark dimension scenario [6]. If a large extra compact space exists, it affects the cosmological history at early times. In particular, the temperature $T_{\rm tmp}$ in the radiation-dominated era can be higher than the compactification scale $m_{\rm KK}$ since the latter has a small value in such a case.

In our previous papers [7,8], we studied the time evolution of the space and the background values of the moduli in a six-dimensional (6D) model compactified on a sphere S^2 by solving the 6D field equations numerically.[1] We found that when the initial temperature of the universe is higher than $m_{\rm KK}$, the expansion rate for the three-dimensional (3D) noncompact space deviates from that of the usual 4D cosmology. In general, the 3D scale factor e^A evolves as $t^{2/(3(1+w))}$, where t is the cosmological time and w is the ratio of the pressure to the energy density. In the radiation-dominated era, w^{-1} measures the dimensions that the radiation feels. In fact, when $T_{\rm tmp} > m_{\rm KK}$, the radiation feels the whole five-dimensional (5D) space and $e^A \propto t^{5/9}$. As the universe expands and the temperature goes down, the radiation gradually ceases to feel the compact space, and w^{-1} approaches to three after $T_{\rm tmp}$ gets lower than $m_{\rm KK}$. Then, the expansion rate slows down to $e^A \propto t^{1/2}$. We also found that even if the moduli are stabilized at the initial time, the moduli oscillation is induced by the pressure for the two-dimensional (2D) compact space $p_2^{\rm rad}$. This effect cannot be discussed in the conventional 4D effective theory approach since $p_2^{\rm rad}$ is absent in the 4D Einstein equation. When $T_{\rm tmp} > m_{\rm KK}$, the effect of $p_2^{\rm rad}$ on the moduli dynamics cannot be neglected. If the lifetime of the moduli is long enough, the induced moduli oscillation eventually dominates the energy density

*otsuka.hajime@phys.kyushu-u.ac.jp
†sakamura@post.kek.jp

[1]This model is basically based on a gauged 6D supergravity on S^2 [9], which has many interesting properties, e.g., a self-tuning of the four-dimensional (4D) vacuum energy [4,10–12] and a verification of swampland conjecture [13]. Its string realization is also discussed in Ref. [14].

and the 3D space expands as $e^A \propto t^{2/3}$ at later times. Therefore, there are the following eras in this setup.

(1) 6D radiation-dominated era ($e^A \propto t^{5/9}$)
(2) 4D radiation-dominated era ($e^A \propto t^{1/2}$)
(3) (Induced) moduli-oscillation-dominated era ($e^A \propto t^{2/3}$)

The era 3 will end by the decay of the moduli, and transition into the 4D radiation-dominated era again [15]. After that, the universe behaves as the standard cosmology. Let us denote the transition time from the era 1 to the era 2 as $t_{\rm rad}$, and that from 2 to 3 as $t_{\rm mod}$. In principle, the spacetime evolution is determined once the model parameters and the initial conditions are provided. However, since these results are obtained by the numerical computations in the previous works, we cannot directly see how the transition times $t_{\rm rad}$ and $t_{\rm mod}$ depend on the initial parameters. Besides, it is difficult to pursue the whole history of the universe due to the limitation of the computational power.

In this paper, we derive approximate expressions for the 3D scale factor, the moduli background values and the transition times in terms of analytic functions by solving the 6D evolution equations under some approximations. Since we can discriminate the eras by the power p, which is defined as $e^A \propto t^p$ in each era, we will focus on the change of p during the spacetime evolution. The expressions derived in this paper enable us to pursue the spacetime evolution until much later times than the previous works, and to clarify the dependence of the transition times $t_{\rm rad}$ and $t_{\rm mod}$ on the model parameters and the initial temperature. These results will help make discussions transparent.

The paper is organized as follows. In Sec. II, we briefly explain our setup and show the evolution equations. In Sec. III, we derive analytic expressions for various quantities by solving the evolution equations under some plausible approximations. We then define the effective power p and derive its explicit expression using the functions we have defined. In Sec. IV, we discuss the time evolution of p, and estimate the transition times. Section V devoted to the summary. In Appendix A, brief derivations of the energy density and the pressures for the radiation are shown. In Appendix B, we derive the evolution equation for the temperature from the conservation law of the energy-momentum tensor. In Appendix C, we provide a general solution to the inhomogeneous differential equation that describes the moduli oscillation.

II. SETUP

We consider a 6D model used in our previous works [7,8]. In this section, we briefly review the model and the evolution equations for the universe. The spacetime is compactified on a 2D sphere S^2. As coordinates on S^2, we choose the spherical ones $(x^4, x^5) = (\theta, \phi)$, where θ and ϕ are the polar and the azimuthal angles, respectively.

The action is given by[2]

$$S = \int d^6x \sqrt{-g^{(6)}} \left\{ -\frac{1}{2}R^{(6)} - \frac{1}{2}\partial^M\sigma\partial_M\sigma - \frac{g_{\rm gc}^2 e^\sigma}{4} \times F^{MN}F_{MN} - V_{\rm pot}(\sigma) \right\}, \tag{2.1}$$

where $M, N = 0, 1, \ldots, 5$ denote the 6D indices, $g^{(6)}$ is the determinant of the 6D metric tensor, $R^{(6)}$ is the 6D Ricci scalar, σ is a real scalar, $F_{MN} \equiv \partial_M A_N - \partial_N A_M$ is the field strength of a U(1) gauge field A_M, and $g_{\rm gc}$ is the gauge coupling constant. The scalar potential $V_{\rm pot}(\sigma)$ is given by

$$V_{\rm pot}(\sigma) = 2e^{-\sigma} + \frac{m^2}{2}(\sigma - \sigma_*)^2, \tag{2.2}$$

where m and σ_* are positive constants.

Except for the second term in (2.2), the action (2.1) can be embedded into a gauged 6D $\mathcal{N} = (1, 0)$ supergravity [9,16]. We add the second term in order to stabilize the moduli completely.

In this paper, we neglect effects of the 3-branes, one of which the standard model particles live,[3] and assume that the background spacetime has homogeneity and isotropy for 3D noncompact space and a spherical symmetry for S^2. Thus, we take the following ansatz for the background fields.

$$g_{MN} = \begin{pmatrix} -1 & & & \\ & e^{2A(t)}1_3 & & \\ & & e^{2B(t)} & \\ & & & e^{2B(t)}\sin^2\theta \end{pmatrix},$$
$$F_{\mu\nu} = F_{\mu\theta} = F_{\mu\phi} = 0,$$
$$F_{\theta\phi} = -F_{\phi\theta} = \frac{\sin\theta}{2g_{\rm gc}}, \qquad F_{\theta\theta} = F_{\phi\phi} = 0,$$
$$\sigma = \sigma(t), \tag{2.3}$$

where $\mu, \nu = 0, 1, 2, 3$ are the 4D indices.

In the absence of the radiation in the bulk, the model has the following static solution.[4]

$$A = 0, \qquad B = B_* \equiv \frac{\sigma_*}{2} - \ln 2, \qquad \sigma = \sigma_*, \tag{2.4}$$

[2]Throughout the paper except for Secs. IV B and IV C, we work in the 6D Planck unit $M_6 = 1$, where M_6 is the 6D Planck mass.

[3]See for more details about codimension-two branes [17–19].

[4]Throughout the paper, we normalize the 3D scale factor as $A(t = 0) = 0$.

and the Kaluza-Klein (KK) mass scale is given by[5]

$$m_{\rm KK} \equiv e^{-B_*} = 2e^{-\sigma_*/2}. \tag{2.5}$$

In addition to the above field content, we introduce the radiation in the bulk. In 6D $\mathcal{N}=1$ supergravity, the number of hypermultiplets n_H and that of vector multiplets n_V are constrained by the anomaly cancellation condition $n_H - n_V = 244$ [16,20,21].[6] Therefore, at least 245 hypermultiplets exist in the bulk. Since each hypermultiplet has 4 bosonic and 4 fermionic degrees of freedom, we assume that the degrees of freedom for the radiation is $g_{\rm dof} = 2000$ in this paper. Due to the isometries of the spacetime, the energy-momentum tensor for the radiation has the form of

$$(T^{\rm rad})^N_M = \begin{pmatrix} \rho^{\rm rad} & & & \\ & -p_3^{\rm rad} 1_3 & & \\ & & -p_2^{\rm rad} & \\ & & & -p_2^{\rm rad}\sin^2\theta \end{pmatrix}, \tag{2.6}$$

where $\rho^{\rm rad}$, $p_3^{\rm rad}$, and $p_2^{\rm rad}$ are the radiation energy density, the pressures in the noncompact 3D space and in the compact 2D space, respectively. Their explicit forms are listed in Appendix A.

In the presence of the radiation, the static solution (2.4) is no longer a solution of the field equations, and the universe continues to expand. Substituting the background ansatz (2.3) and (2.6) into the 6D Einstein equations and the dilaton field equation, we obtain the evolution equations for the background fields, which are summarized as

$$\begin{aligned}
\ddot{A} &= -(3\dot{A}+2\dot{B})\dot{A} + \left(e^{-\sigma} - \frac{e^{\sigma-4B}}{16}\right) + \frac{m^2}{4}(\sigma-\sigma_*)^2 + p_3^{\rm rad},\\
\ddot{B} &= -(3\dot{A}+2\dot{B})\dot{B} + \left(e^{-\frac{\sigma}{2}} - \frac{e^{\frac{\sigma}{2}-2B}}{4}\right)\\
&\quad\times\left(e^{-\frac{\sigma}{2}} - \frac{3e^{\frac{\sigma}{2}-2B}}{4}\right) + \frac{m^2}{4}(\sigma-\sigma_*)^2 + p_2^{\rm rad},\\
\ddot{\sigma} &= -(3\dot{A}+2\dot{B})\dot{\sigma} + 2\left(e^{-\sigma} - \frac{e^{\sigma-4B}}{16}\right) - m^2(\sigma-\sigma_*),
\end{aligned} \tag{2.7}$$

with the constraint,

$$\begin{aligned}
3\dot{A}^2 + \dot{B}^2 + 6\dot{A}\,\dot{B} - \frac{1}{2}\dot{\sigma}^2 &= 2\left(e^{-\frac{\sigma}{2}} - \frac{e^{\frac{\sigma}{2}-2B}}{4}\right)^2\\
&\quad + \frac{m^2}{2}(\sigma-\sigma_*)^2 + \rho^{\rm rad}\\
&\equiv \hat{\rho}^{\rm tot}.
\end{aligned} \tag{2.8}$$

We have used the relation (A11).

The energy density and the pressures are expressed as (see Appendix A)[7]

$$\begin{aligned}
\rho^{\rm rad} &= \frac{g_{\rm dof}e^{-2B}}{8\pi^3\beta^4}\left(\frac{\pi^4}{16} + 3Q_1 + Q_2\right),\\
p_3^{\rm rad} &= \frac{g_{\rm dof}e^{-2B}}{8\pi^3\beta^4}\left(\frac{\pi^4}{48} + Q_1\right),\\
p_2^{\rm rad} &= \frac{g_{\rm dof}e^{-2B}}{16\pi^3\beta^4}Q_2,
\end{aligned} \tag{2.9}$$

where $\beta \equiv 1/T_{\rm tmp}$ is the inverse temperature, the functions $Q_1(x)$ and $Q_2(x)$ are defined in (A6) and (A8) respectively, and their arguments are $e^{-B}\beta$. The evolution equation for β is obtained from the conservation law for the energy-momentum tensor as

$$\frac{\dot{\beta}}{\beta} = \frac{3\dot{A}(\frac{\pi^4}{12} + 4Q_1 + Q_2) + \dot{B}(2Q_2 + Q_3)}{\frac{\pi^4}{4} + 12Q_1 + 5Q_2 + Q_3}, \tag{2.10}$$

where $Q_3(x)$ is defined in (B6). (See Appendix B.) The profiles of $x^2Q_i(x)$ $(i = 1, 2, 3)$ are shown in Fig. 16.

We consider a situation that the moduli B and σ have already been stabilized at $t = 0$. Hence, we choose the initial conditions at $t = 0$ as

$$\begin{aligned}
&A(0) = 0, \quad B(0) = B_*, \quad \sigma(0) = \sigma_*, \quad \beta(0) = \beta_{\rm I},\\
&\dot{A}(0) = \sqrt{\frac{\hat{\rho}^{\rm tot}(0)}{3}}, \quad \dot{B}(0) = \dot{\sigma}(0) = 0,
\end{aligned} \tag{2.11}$$

where $\beta_{\rm I}$ is a positive constant. The value of $\dot{A}(0)$ is determined by the constraint (2.8).

III. INDUCED MODULI OSCILLATION AND 3D SCALE FACTOR

A. Moduli oscillation induced by $p_2^{\rm rad}$

As pointed out in our previous work [8], the pressure for the compact space S^2, $p_2^{\rm rad}$, pushes out the moduli from the potential minimum, and induces an oscillation of the moduli around the stabilized values in (2.4). Namely, even in the case that the moduli have been settled at the stabilized

[5]The mass eigenvalues for the KK gravitons are expressed as $\sqrt{l(l+1)}m_{\rm KK}$, where l is a non-negative integer.

[6]The number of tensor multiplets is assumed to be one, otherwise the theory cannot be described by the Lagrangian.

[7]To simplify the discussion, we assume that the chemical potential μ is negligible, i.e., $\beta\mu \ll 1$, and the radiation consists of bosons and fermions with the same degrees of freedom.

point before the radiation-dominated era, they will start to oscillate again. This effect cannot be neglected if the temperature is high enough compared to $m_{\rm KK}$.

In order to see this behavior, we will see the time evolution of the moduli at early times. We assume that the radiation dominates the energy density at $t=0$, and the initial temperature is higher than $m_{\rm KK}$ (i.e., $\hat{\beta}_{\rm I} \equiv e^{-B_*}\beta_{\rm I} \ll 1$). Since we are interested in the oscillation around the stabilized values in (2.4), we define $\tilde{B} \equiv B - B_*$ and $\tilde{\sigma} \equiv \sigma - \sigma_*$. The mass eigenstates are linear combinations of them, which are defined as

$$\begin{aligned} \varphi_1 &\equiv e^{\frac{3}{2}A}(2\cos\theta\tilde{B} + \sin\theta\tilde{\sigma}), \\ \varphi_2 &\equiv e^{\frac{3}{2}A}(-2\sin\theta\tilde{B} + \cos\theta\tilde{\sigma}). \end{aligned} \tag{3.1}$$

The evolution equations for them are derived from (2.7) as

$$\begin{pmatrix} \ddot{\varphi}_1 \\ \ddot{\varphi}_2 \end{pmatrix} = -\begin{pmatrix} \lambda_1 & \\ & \lambda_2 \end{pmatrix}\begin{pmatrix} \varphi_1 \\ \varphi_2 \end{pmatrix} + 2e^{\frac{3}{2}A}p_2^{\rm rad}\begin{pmatrix} \cos\theta \\ -\sin\theta \end{pmatrix} + \cdots, \tag{3.2}$$

where the ellipsis denotes higher order terms in φ_1 or φ_2, and

$$\begin{aligned} \lambda_1 &\equiv \frac{1}{2}\left(2m_{\rm KK}^2 + m^2 - \sqrt{4m_{\rm KK}^4 + m^4}\right), \\ \lambda_2 &\equiv \frac{1}{2}\left(2m_{\rm KK}^2 + m^2 + \sqrt{4m_{\rm KK}^4 + m^4}\right), \\ \theta &\equiv \tan^{-1}\frac{2m_{\rm KK}^2}{m^2 + \sqrt{4m_{\rm KK}^4 + m^4}} = \tan^{-1}\frac{m_{\rm KK}^2}{\lambda_2 - m_{\rm KK}^2}. \end{aligned} \tag{3.3}$$

We have neglected terms involving $\ddot{A}$, which are assumed to be small at initial times. When $m^2 \gg m_{\rm KK}^2$, for example, these become $\lambda_1 \simeq m_{\rm KK}^2$, $\lambda_2 \simeq m^2$ and $\theta \simeq \lambda_1/\lambda_2$.

In general, it is hard to solve (2.7) analytically because A, B and σ are coupled to each other. However, due to the assumption that the radiation is dominated at initial times, the expansion of the 3D space is determined only by $\rho^{\rm rad}$, and is almost independent of the moduli. Hence we can treat the 3D expansion and the moduli oscillation separately. In fact, from (A13) and (B7), the energy density and the pressure for the compact space S^2 are approximately written as

$$\rho^{\rm rad} \simeq \frac{10 g_{\rm dof}}{\pi^3\beta^6}, \qquad p_2^{\rm rad} \simeq \frac{2g_{\rm dof}}{\pi^3\beta^6}, \tag{3.4}$$

which are independent of the moduli. Notice that $\dot{A} \gg |\dot{B}|$ at the very early times because of the initial condition (2.11). Then, from (2.10) and (B7), we obtain

$$\frac{\dot{\beta}}{\beta} \simeq \frac{3}{5}\dot{A}, \tag{3.5}$$

which is immediately solved as $\beta \simeq \beta_{\rm I} e^{\frac{3}{5}A}$. Thus, (3.4) is rewritten as

$$\rho^{\rm rad} \simeq D_{\rm rad} e^{-\frac{18}{5}A}, \qquad p_2^{\rm rad} \simeq \frac{D_{\rm rad}}{5} e^{-\frac{18}{5}A}, \tag{3.6}$$

where $D_{\rm rad} \equiv 10 g_{\rm dof}/(\pi^3\beta_{\rm I}^6)$.

From (2.8), we have

$$\dot{A} \simeq \sqrt{\frac{\rho^{\rm rad}}{3}} \simeq \sqrt{\frac{D_{\rm rad}}{3}} e^{-\frac{9}{5}A}, \tag{3.7}$$

which leads to

$$t \simeq \int_0^A dx \sqrt{\frac{3}{D_{\rm rad}}} e^{\frac{9}{5}x} = \frac{5}{3\sqrt{3D_{\rm rad}}}(e^{\frac{9}{5}A} - 1). \tag{3.8}$$

Therefore, we have

$$e^A \simeq (1 + \sqrt{C_A}t)^{5/9}, \quad \beta \simeq e^{\frac{3}{5}A} \simeq (1 + \sqrt{C_A}t)^{1/3}, \tag{3.9}$$

where $C_A \equiv (27/25)D_{\rm rad} = 54 g_{\rm dof}/(5\pi^3\beta_{\rm I}^6)$. This approximation is valid when $\hat{\beta} \equiv e^{-B_*}\beta < 1$. This condition is translated as

$$t < t_1 \equiv \frac{1}{\sqrt{C_A}\hat{\beta}_{\rm I}^3} = e^{3B_*}\sqrt{\frac{5\pi^3}{54 g_{\rm dof}}} = 0.038 e^{3B_*}. \tag{3.10}$$

We have used that $\hat{\beta}_{\rm I} \ll 1$.

Using (3.9), (3.2) is rewritten as

$$\begin{pmatrix} \ddot{\varphi}_1 \\ \ddot{\varphi}_2 \end{pmatrix} \simeq -\begin{pmatrix} \lambda_1 & \\ & \lambda_2 \end{pmatrix}\begin{pmatrix} \varphi_1 \\ \varphi_2 \end{pmatrix} + \frac{2D_{\rm rad}}{5}(1 + C_A t)^{-7/6}\begin{pmatrix} \cos\theta \\ -\sin\theta \end{pmatrix}. \tag{3.11}$$

From (2.11), the initial conditions at $t=0$ are read off as

$$\varphi_1(0) = \varphi_2(0) = \dot{\varphi}_1(0) = \dot{\varphi}_2(0) = 0. \tag{3.12}$$

The solution is expressed as

$$\begin{aligned} \varphi_1(t) &\simeq -\frac{2D_{\rm rad}\cos\theta}{5\lambda_1}\left(\frac{\lambda_1}{C_A}\right)^{\frac{7}{12}} {\rm Im}\{e^{\frac{\pi}{12}i}\mathcal{U}_{7/6}(t;\lambda_1,C_A)\} \\ &= -\frac{10\cos\theta}{27}\left(\frac{C_A}{\lambda_1}\right)^{\frac{5}{12}} {\rm Im}\{e^{\frac{\pi}{12}i}\mathcal{U}_{7/6}(t;\lambda_1,C_A)\}, \\ \varphi_2(t) &\simeq \frac{2D_{\rm rad}\sin\theta}{5\lambda_2}\left(\frac{\lambda_2}{C_A}\right)^{\frac{7}{12}} {\rm Im}\{e^{\frac{\pi}{12}i}\mathcal{U}_{7/6}(t;\lambda_2,C_A)\} \\ &= \frac{10\sin\theta}{27}\left(\frac{C_A}{\lambda_2}\right)^{\frac{5}{12}} {\rm Im}\{e^{\frac{\pi}{12}i}\mathcal{U}_{7/6}(t;\lambda_2,C_A)\}. \end{aligned} \tag{3.13}$$

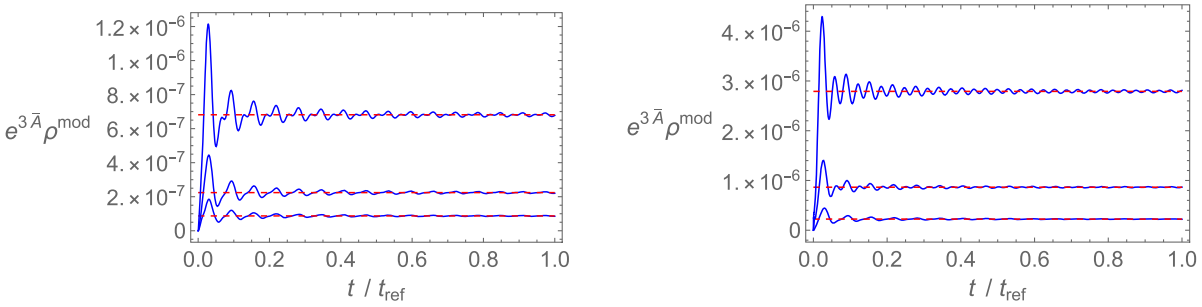

FIG. 1. The profiles of $e^{3\bar{A}}\rho^{\rm mod}$ as a function of $t/t_{\rm ref}$, where $t_{\rm ref} \equiv 100/\sqrt{\lambda_1}$. In the left plot, we choose $\sigma_* = 10, 12, 14$ from bottom to top with $m = 10^{-2}$ and $\beta_{\rm I} = 20$. In the right plot, we choose $m = 10^{-2}, 10^{-3}, 10^{-4}$ from bottom to top with $\sigma_* = 12$ and $\beta_{\rm I} = 20$. The dashed lines denote the asymptotic values given by (3.19).

(See Appendix C.) The function $\mathcal{U}_q(t;\lambda,C)$ is defined by the incomplete gamma function as (C7). From these and (3.9), we obtain an approximate solution of the moduli evolution equations at early times. We have checked that this approximate solution well agrees with the solution of the full evolution equation (2.7) obtained by the numerical computation.

As we will see in the next subsection, it is convenient to define

$$\bar{A}(t) \equiv A(t) + \tilde{B}(t). \tag{3.14}$$

Since $|\tilde{B}(t)| \ll A(t)$ except for an early short period $0 \le t \ll C_A^{-1/2}$, $e^{\bar{A}}$ can be understood as a modified 3D scale factor. The mixing term between $\dot{A}$ and $\dot{B}$ in the constraint (2.8) is absorbed into $\dot{\bar{A}}^2$, and (2.8) is rewritten in a similar form to the 4D Friedmann equation.[8]

$$3\dot{\bar{A}}^2 = \rho^{\rm mod} + \rho^{\rm rad}, \tag{3.15}$$

where

$$\rho^{\rm mod} \equiv 2\dot{B}^2 + \frac{1}{2}\dot{\sigma}^2 + 2\left(e^{-\frac{q}{2}} - \frac{e^{\frac{q}{2}-2B}}{4}\right)^2 + \frac{m^2}{2}(\sigma-\sigma_*)^2, \tag{3.16}$$

represents the energy density of the moduli oscillation. The moduli energy density $\rho^{\rm mod}$ is expressed in terms of φ_1 and φ_2 as

$$\rho^{\rm mod} = \frac{e^{-3\bar{A}}}{2}\left\{\left(\dot{\varphi}_1 - \frac{3}{2}\dot{\bar{A}}\varphi_1\right)^2 + \left(\dot{\varphi}_2 - \frac{3}{2}\dot{\bar{A}}\varphi_2\right)^2 + \lambda_1\varphi_1^2 + \lambda_2\varphi_2^2\right\} + \cdots, \tag{3.17}$$

where the ellipsis denotes higher order terms in φ_1 or φ_2. Using (3.13), we can plot $e^{3\bar{A}}\rho^{\rm mod}(t)$ as Fig. 1. From this plot, we can see that $e^{3\bar{A}}\rho^{\rm mod}$ is almost a constant for $t > t_{\rm ref}$, where

$$t_{\rm ref} \equiv \frac{100}{\sqrt{\lambda_1}} \sim 100\max\left(\frac{\sqrt{2}}{m}, \frac{1}{m_{\rm KK}}\right). \tag{3.18}$$

Noting that $|\Gamma(1-q, ix)| \simeq x^{-q}$ for $x \gg 1$, we find that

$$\lim_{t\to\infty} e^{3\bar{A}(t)}\rho^{\rm mod}(t) = \frac{50C_A^{5/6}}{729}\left(\lambda_1^{1/6}\cos^2\theta\left|\Gamma\left(-\frac{1}{6}, i\sqrt{\frac{\lambda_1}{C_A}}\right)\right|^2 + \lambda_2^{1/6}\sin^2\theta\left|\Gamma\left(-\frac{1}{6}, i\sqrt{\frac{\lambda_2}{C_A}}\right)\right|^2\right) \equiv C_{\rm mod}. \tag{3.19}$$

We have used (C8). Namely, $\rho^{\rm mod}$ decays as

$$\rho^{\rm mod}(t) \simeq C_{\rm mod}e^{-3\bar{A}(t)}. \tag{3.20}$$

at late times ($t > t_{\rm ref}$).

[8]Note that $\dot{\bar{A}}$ corresponds to the Hubble expansion rate.

Here we comment on the validity of the above approximations. We have used that $\rho^{\rm rad} \gg \rho^{\rm mod}$ to obtain (3.9). When this condition is satisfied, the ratio of $\rho^{\rm mod}$ to $\rho^{\rm rad}$ is

$$\frac{\rho^{\rm mod}}{\rho^{\rm rad}} \simeq \frac{27}{25C_A}\left\{\left(\dot{\varphi}_1 - \frac{3}{2}\dot{\bar{A}}\varphi_1\right)^2 + \left(\dot{\varphi}_2 - \frac{3}{2}\dot{\bar{A}}\varphi_2\right)^2 + \lambda_1\varphi_1^2 + \lambda_2\varphi_2^2\right\}(1+\sqrt{C_A}t)^{\frac{1}{3}} \equiv r_{\rm m/r}(t), \tag{3.21}$$

where $\varphi_1(t)$ and $\varphi_2(t)$ are given by (3.13), and $\dot{\bar{A}}(t) = 5\sqrt{C_A}/\{9(1+\sqrt{C_A}t)\}$. Note that the function $r_{\rm m/r}(t)$ is determined when the model parameters m, σ_* and the initial condition $\beta_{\rm I}$ are given. This ratio is plotted in Fig. 2. We can see from the plots that the approximate solution in (3.13) is no longer valid when $t \simeq t_{\rm ref}$ in the case of $\beta_{\rm I} = 10$, $m = 0.01$ and $\sigma_* = 14$. As a general property, the ratio $\rho^{\rm mod}/\rho^{\rm rad}$ takes a larger value for higher initial temperature or for shallower moduli potential (i.e., smaller m or larger σ_*). When $\rho^{\rm mod}$ approaches to $\rho^{\rm rad}$, the expansion rate for the 3D space becomes larger than (3.7), and the inhomogeneous term in (3.2) decays more rapidly than (3.11). After the inhomogeneous term becomes negligible, the solution will reduce to a linear combination of two simple harmonic oscillators, and $e^{3A}\rho^{\rm mod}$ becomes constant. Thus, the constant $C_{\rm mod}$ in (3.20) takes a smaller value than (3.19) if $r_{\rm m/r}$ is close to one before $t = t_{\rm ref}$.

B. Smoothed 3D scale factor

In the usual 4D cosmology, the 3D scale factor evolves as $e^{A(t)} \propto t^{1/2}$ in the radiation-dominated era and as $e^{A(t)} \propto t^{2/3}$ in the matter-dominated era. Thus, it is convenient to define the effective power p as $p \equiv t\dot{A}$. Then, $p = 1/2$ $(2/3)$ in the radiation- (matter-) dominated era. However, as we pointed out in Ref. [8], this quantity oscillates due to the effect of the moduli oscillation (see Fig. 3). Thus we modify the definition of p as

$$p \equiv (t - t_{\rm c})\dot{\bar{A}}, \tag{3.22}$$

where $\bar{A}$ is defined by (3.14). The constant $t_{\rm c}$ is chosen so that p is almost independent of t at early times. We will show how to choose $t_{\rm c}$ in Sec. III D. As we can see from Fig. 3, this modification removes the effect of the moduli oscillation [8].

For $t \geq t_{\rm ref}$, the radiation energy density in (2.9) is approximated as

$$\rho^{\rm rad} \simeq C_{\rm rad}\frac{v_\rho(\hat{\beta})}{\hat{\beta}^6}, \qquad C_{\rm rad} \equiv \frac{g_{\rm dof}e^{-6B_*}}{8\pi^3}, \tag{3.23}$$

where $\hat{\beta} \equiv e^{-B_*}\beta = m_{\rm KK}\beta$ is the inverse temperature in the unit of the KK mass $m_{\rm KK}$, and

$$v_\rho(x) \equiv x^2\left\{\frac{\pi^4}{16} + 3Q_1(x) + Q_2(x)\right\}. \tag{3.24}$$

The evolution equation for β (2.10) is approximated as

$$\frac{\dot{\beta}}{\beta} \simeq v_\beta(\hat{\beta})\dot{\bar{A}}, \tag{3.25}$$

where

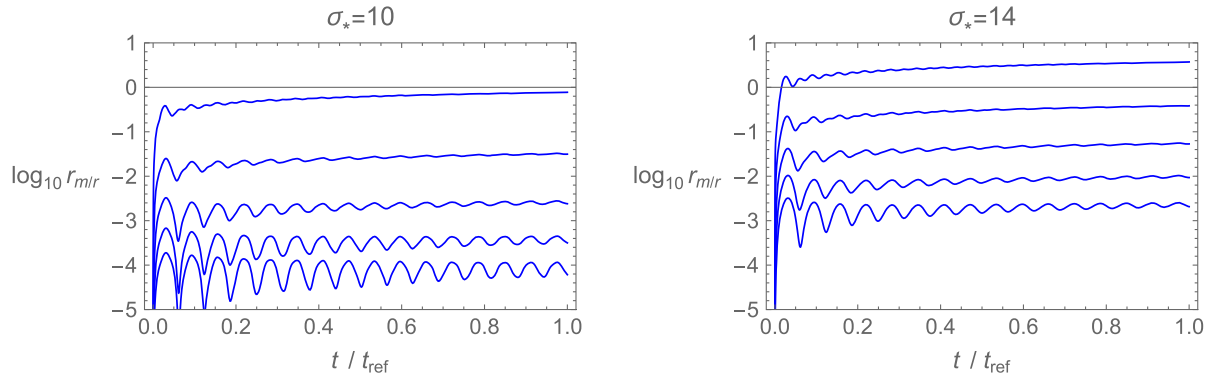

FIG. 2. The logarithm of the function $r_{\rm m/r}$ in (3.21) as a function of $t/t_{\rm ref}$. The lines corresponds $\beta_{\rm I} = 10, 20, 30, 40, 50$ from top to bottom. The other parameters are chosen as $m = 0.01$, $\sigma_* = 10$ (left plot), and $\sigma_* = 14$ (right plot).

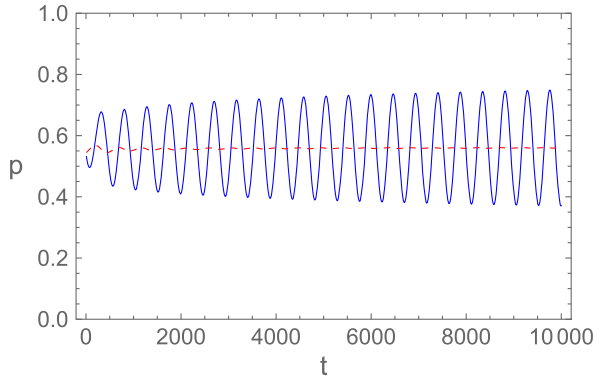

FIG. 3. The profiles of $(t-t_c)\dot{A}(t)$ (solid line) and $p(t)$ defined in (3.22) (dashed line) in the case of $m=0.1$, $\sigma_*=10$, $\beta_I=10$, and $t_c=-125$ in the unit of M_6.

$$v_\beta(x) \equiv \frac{\frac{\pi^4}{4}+12Q_1(x)+3Q_2(x)}{\frac{\pi^4}{4}+12Q_1(x)+5Q_2(x)+Q_3(x)}. \tag{3.26}$$

The profiles of $v_\beta(x)$ and $v_\rho(x)$ are shown in Fig. 4.

Solving (3.25), the (smoothed) 3D scale factor $\bar{A}$ is expressed as a function of $\hat{\beta}$,

$$\begin{aligned}\bar{A}(\hat{\beta}) &\simeq \bar{A}_{\rm ref}+\int_{\hat{\beta}_{\rm ref}}^{\hat{\beta}}\frac{dx}{xv_\beta(x)}\\ &= \bar{A}_{\rm ref}+\mathcal{F}(\hat{\beta})-\mathcal{F}(\hat{\beta}_{\rm ref}),\end{aligned} \tag{3.27}$$

where $\bar{A}_{\rm ref}$ and $\hat{\beta}_{\rm ref}$ denote the values at $t=t_{\rm ref}$, and

$$\mathcal{F}(x) \equiv \int_1^x \frac{dy}{yv_\beta(y)}. \tag{3.28}$$

The profile of $\mathcal{F}(x)$ is shown in Fig. 5.

C. Expression of effective power p

Here we derive an explicit expression for the effective power p. From (3.15) and (3.20), we have[9]

$$\dot{\bar{A}} \simeq \sqrt{\frac{1}{3}(C_{\rm mod}e^{-3\bar{A}}+\rho^{\rm rad})}, \tag{3.29}$$

which leads to

$$\begin{aligned}t-t_{\rm ref} &\simeq \int_{\hat{\beta}_{\rm ref}}^{\hat{\beta}} dx\frac{d\bar{A}}{d\hat{\beta}}(x)\sqrt{\frac{3}{C_{\rm mod}e^{-3\bar{A}(x)}+\rho^{\rm rad}(x)}}\\ &= \int_{\hat{\beta}_{\rm ref}}^{\hat{\beta}}\frac{dx}{xv_\beta(x)}\sqrt{\frac{3}{C_{\rm mod}e^{-3\bar{A}(x)}+C_{\rm rad}x^{-6}v_\rho(x)}}\\ &= \sqrt{\frac{3}{C_{\rm rad}}}\int_{\hat{\beta}_{\rm ref}}^{\hat{\beta}} dx\frac{x^2}{v_\beta(x)\sqrt{v_\rho(x)}}\{1+R_{\rm rad}^{\rm mod}\mathcal{R}(x)\}^{-1/2},\end{aligned} \tag{3.30}$$

where

$$R_{\rm rad}^{\rm mod} \equiv \frac{C_{\rm mod}e^{-3\bar{A}_{\rm ref}+3\mathcal{F}(\hat{\beta}_{\rm ref})}}{C_{\rm rad}}, \qquad \mathcal{R}(x) \equiv \frac{x^6e^{-3\mathcal{F}(x)}}{v_\rho(x)}. \tag{3.31}$$

We have used (3.27) at the last step. As shown in Fig. 6, $\mathcal{R}(x)$ is well approximated as a linear function.

$$\mathcal{R}(x) \simeq 0.0135x. \tag{3.32}$$

Thus, the above expression can be approximated as

$$t \simeq t_{\rm ref}+\sqrt{\frac{3}{C_{\rm rad}}}\int_{\hat{\beta}_{\rm ref}}^{\hat{\beta}} dx\frac{x^2}{v_\beta(x)\sqrt{v_\rho(x)}}\left(1+\frac{x}{\hat{\beta}_{\rm mod}}\right)^{-1/2}, \tag{3.33}$$

where

$$\hat{\beta}_{\rm mod} \equiv \frac{1}{0.0135R_{\rm rad}^{\rm mod}} \simeq \frac{74.1}{R_{\rm rad}^{\rm mod}}. \tag{3.34}$$

Using this expression, the effective power p defined in (3.22) is expressed as

$$\begin{aligned}p(\hat{\beta}) &= (t-t_c)\frac{d\bar{A}}{d\hat{\beta}}(\hat{\beta})\left\{\frac{dt}{d\hat{\beta}}(\hat{\beta})\right\}^{-1}\\ &\simeq \left\{t_{\rm ref}-t_c+\int_{\hat{\beta}_{\rm ref}}^{\hat{\beta}}\frac{dx}{xv_\beta(x)}\sqrt{\frac{3}{C_{\rm mod}e^{-3\bar{A}(x)}+C_{\rm rad}x^{-6}v_\rho(x)}}\right\}\sqrt{\frac{C_{\rm mod}e^{-3\bar{A}(\hat{\beta})}+C_{\rm rad}\hat{\beta}^{-6}v_\rho(\hat{\beta})}{3}}\\ &\simeq \left\{t_{\rm ref}-t_c+\sqrt{\frac{3}{C_{\rm rad}}}\int_{\hat{\beta}_{\rm ref}}^{\hat{\beta}} dx\frac{x^2}{v_\beta(x)\sqrt{v_\rho(x)}}\left(1+\frac{x}{\hat{\beta}_{\rm mod}}\right)^{-1/2}\right\}\sqrt{\frac{C_{\rm rad}v_\rho(\hat{\beta})}{3\hat{\beta}^6}}\left(1+\frac{\hat{\beta}}{\hat{\beta}_{\rm mod}}\right)^{1/2}.\end{aligned} \tag{3.35}$$

[9]We focus on the positive solution of $\dot{\bar{A}}$ since we are interested in an expanding 3D universe.

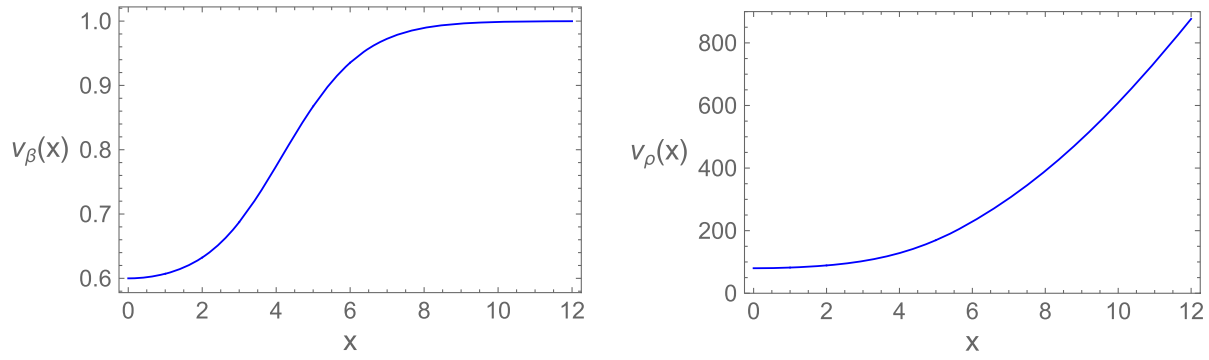

FIG. 4. The profiles of $v_\beta(x)$ and $v_\rho(x)$.

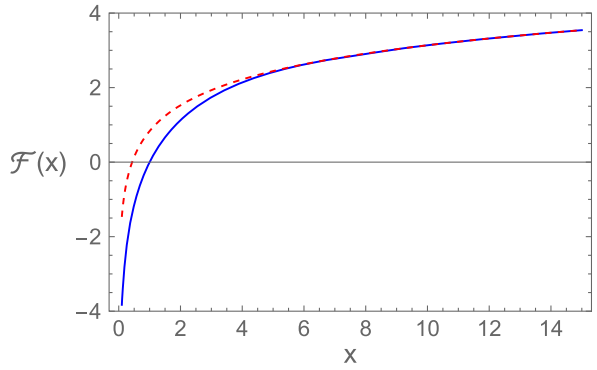

FIG. 5. The profile of $\mathcal{F}(x)$. The dotted line represents $\ln x + 0.833$.

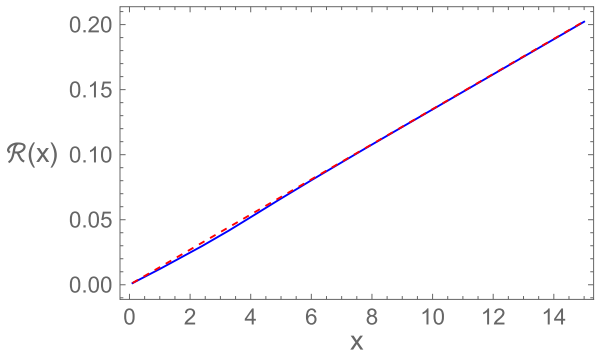

FIG. 6. The profile of $\mathcal{R}(x)$. The dotted represents $0.0135x$.

D. Choice of t_c

As we mentioned, the constant t_c is determined so that p is almost independent of t at early times $t \le t_{\rm ref}$. By assumption, $\rho^{\rm mod}(t_{\rm ref}) \simeq C_{\rm mod} e^{-3\bar{A}_{\rm ref}} \ll \rho^{\rm rad}(t_{\rm ref}) \simeq C_{\rm rad}\hat{\beta}_{\rm ref}^{-6} v_\rho(\hat{\beta}_{\rm ref})$, i.e., $\hat{\beta}_{\rm ref} \ll \hat{\beta}_{\rm mod}$. Then, when $t \sim t_{\rm ref}$, (3.33) is approximated as

$$t(\hat{\beta}) = t_{\rm ref} + \sqrt{\frac{3}{C_{\rm rad}}}\int_{\hat{\beta}_{\rm ref}}^{\hat{\beta}} dx \frac{x^2}{v_\beta(x)\sqrt{v_\rho(x)}} \times \left(1 - \frac{x}{2\hat{\beta}_{\rm mod}} + \cdots\right) \simeq t_{\rm ref} + \sqrt{\frac{3}{C_{\rm rad}}}\left[\mathcal{G}(x) - \frac{1}{2\hat{\beta}_{\rm mod}}\mathcal{H}(x)\right]_{\hat{\beta}_{\rm ref}}^{\hat{\beta}}, \tag{3.36}$$

where

$$\mathcal{G}(x) \equiv \int_0^x dy \frac{y^2}{v_\beta(y)\sqrt{v_\rho(y)}}, \qquad \mathcal{H}(x) \equiv \int_0^x dy \frac{y^3}{v_\beta(y)\sqrt{v_\rho(y)}}. \tag{3.37}$$

Figure 7 shows the profiles of $\mathcal{G}(x)/x^2$ and $\mathcal{H}(x)/x^3$.

Thus, when $t \sim t_{\rm ref}$, (3.35) is approximated as

$$p(\hat{\beta}) \simeq \left\{ t_{\rm ref} - t_{\rm c} + \sqrt{\frac{3}{C_{\rm rad}}}\left[\mathcal{G}(x) - \frac{1}{2\hat{\beta}_{\rm mod}}\mathcal{H}(x)\right]_{\hat{\beta}_{\rm ref}}^{\hat{\beta}} \right\} \times \sqrt{\frac{C_{\rm rad} v_\rho(\hat{\beta})}{3\hat{\beta}^6}}\left(1 + \frac{\hat{\beta}}{2\hat{\beta}_{\rm mod}}\right). \tag{3.38}$$

Here we choose $t_{\rm c}$ as

$$t_{\rm c} = t_{\rm ref} - \sqrt{\frac{3}{C_{\rm rad}}}\left\{\mathcal{G}(\hat{\beta}_{\rm ref}) - \frac{1}{2\hat{\beta}_{\rm mod}}\mathcal{H}(\hat{\beta}_{\rm ref})\right\}. \tag{3.39}$$

Then, (3.38) becomes

$$p(\hat{\beta}) \simeq \left\{\mathcal{G}(\hat{\beta}) - \frac{1}{2\hat{\beta}_{\rm mod}}\mathcal{H}(\hat{\beta})\right\}\frac{\sqrt{v_\rho(\hat{\beta})}}{\hat{\beta}^3}\left(1 + \frac{\hat{\beta}}{2\hat{\beta}_{\rm mod}}\right). \tag{3.40}$$

For $\hat{\beta} \ll 1$, the functions we have defined behave as

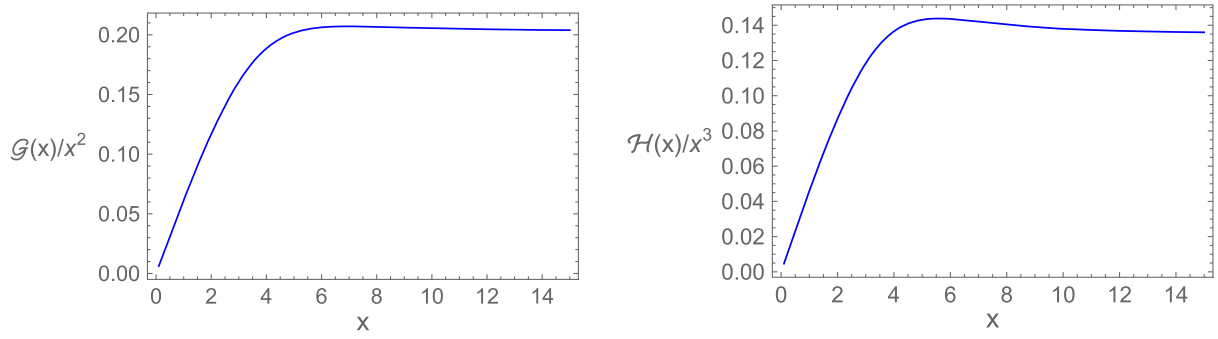

FIG. 7. The profiles of $\mathcal{F}(x)$, $\mathcal{G}(x)/x^2$ and $\mathcal{H}(x)/x^3$.

$$v_\beta(\hat{\beta}) \simeq \frac{3}{5}, \quad v_\rho(\hat{\beta}) \simeq 80,$$
$$\mathcal{F}(\hat{\beta}) \simeq \frac{5}{3}\ln\hat{\beta}, \quad \mathcal{G}(\hat{\beta}) \simeq \frac{\sqrt{5}}{36}\hat{\beta}^3, \quad \mathcal{H}(\hat{\beta}) \simeq \frac{\sqrt{5}}{48}\hat{\beta}^4. \tag{3.41}$$

By assumption, $\hat{\beta} \ll \hat{\beta}_{\rm mod}$. Thus, $p(\hat{\beta})$ behaves as[10]

$$p(\hat{\beta}) \simeq \mathcal{G}(\hat{\beta})\frac{\sqrt{v_\rho(\hat{\beta})}}{\hat{\beta}^3} \simeq \frac{5}{9}, \tag{3.42}$$

which is independent of $\hat{\beta}$ (or t). Hence the choice of t_0 in (3.39) is appropriate.

Using this choice of t_0, (3.35) becomes

$$p(\hat{\beta}) \simeq \left\{\int_{\hat{\beta}_{\rm ref}}^{\hat{\beta}} dx \frac{x^2}{v_\beta(x)\sqrt{v_\rho(x)}}\left(1+\frac{x}{\hat{\beta}_{\rm mod}}\right)^{-1/2} + \mathcal{G}(\hat{\beta}_{\rm ref}) - \frac{\mathcal{H}(\hat{\beta}_{\rm ref})}{2\hat{\beta}_{\rm mod}}\right\} \times \frac{\sqrt{v_\rho(\hat{\beta})}}{\hat{\beta}^3}\left(1+\frac{\hat{\beta}}{\hat{\beta}_{\rm mod}}\right)^{1/2}. \tag{3.43}$$

Combining this with (3.33), we can plot p as a function of t.

IV. TIME EVOLUTION OF 3D SPACE

In this section, we discuss the expansion of the 3D space by evaluating the time evolution of the effective power p.

A. Parameter dependence of effective power p

When $\hat{\beta} \ll \hat{\beta}_{\rm mod}$, (3.33) and (3.43) reduce to

$$t(\hat{\beta}) \simeq t_{\rm ref} + \sqrt{\frac{3}{C_{\rm rad}}}\{\mathcal{G}(\hat{\beta}) - \mathcal{G}(\hat{\beta}_{\rm ref})\},$$
$$p(\hat{\beta}) \simeq \mathcal{G}(\hat{\beta})\frac{\sqrt{v_\rho(\hat{\beta})}}{\hat{\beta}^3}. \tag{4.1}$$

From Fig. 8, we can see that the power p changes its value from $9/5$ to $1/2$ during the period $2 < \hat{\beta} < 10$. If $\hat{\beta}_{\rm mod} \gg 15$, the 3D space expands as in the 4D radiation-dominated era until $\hat{\beta}$ approaches to $\hat{\beta}_{\rm mod}$.

When $\hat{\beta} \gg \hat{\beta}_{\rm mod}$, on the other hand, the contribution of the moduli oscillation dominates the energy density, and $p(\hat{\beta})$ in (3.43) can be estimated as

$$t(\hat{\beta}) \simeq t_{\rm ref} + \sqrt{\frac{3}{C_{\rm rad}}}\int_{\hat{\beta}_{\rm ref}}^{\hat{\beta}} dx \frac{x^2}{v_\beta(x)\sqrt{v_\rho(x)}}\sqrt{\frac{\hat{\beta}_{\rm mod}}{x}} \simeq t_{\rm ref} + \sqrt{\frac{3\hat{\beta}_{\rm mod}}{C_{\rm rad}}}\int_0^{\hat{\beta}} dx \frac{x^{3/2}}{\frac{\pi^2}{4}x} = t_{\rm ref} + \frac{8}{3\pi^2}\sqrt{\frac{3\hat{\beta}_{\rm mod}}{C_{\rm rad}}}\hat{\beta}^{3/2},$$
$$p(\hat{\beta}) \simeq \left\{\int_0^{\hat{\beta}} dx \frac{x^{3/2}}{v_\beta(x)\sqrt{v_\rho(x)}}\right\}\frac{\sqrt{v_\rho(\hat{\beta})}}{\hat{\beta}^{5/2}} \simeq \left\{\int_0^{\hat{\beta}} dx \frac{x^{3/2}}{\frac{\pi^2}{4}x}\right\}\frac{\frac{\pi^2}{4}\hat{\beta}}{\hat{\beta}^{5/2}} = \frac{2}{3}, \tag{4.2}$$

where we have used that

$$v_\beta(x) \simeq 1, \qquad v_\rho(x) \simeq \frac{\pi^4}{16}x^2, \tag{4.3}$$

for $x \gg 1$.

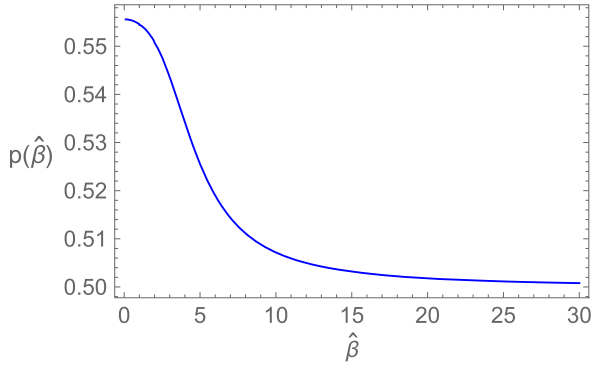

FIG. 8. The profile of the function in (4.1).

[10]This value corresponds to the 6D radiation-dominated universe, which is also obtained from $e^A \propto t^{2/(3(1+w))}$ with $w = 1/5$. Note that w^{-1} measures the space dimensions that the radiation feels.

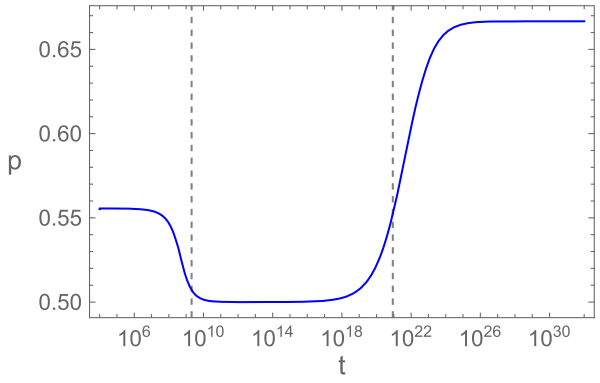

FIG. 9. The effective power p as a function of t. The parameters are chosen as $\sigma_* = 14$, $\hat{\beta}_{\rm ref} = 10^{-2}$ and $R_{\rm rad}^{\rm mod} = 10^{-5}$. The left and right vertical dashed lines denotes $t = t_{\rm rad}$ and $t = t_{\rm mod}$, respectively.

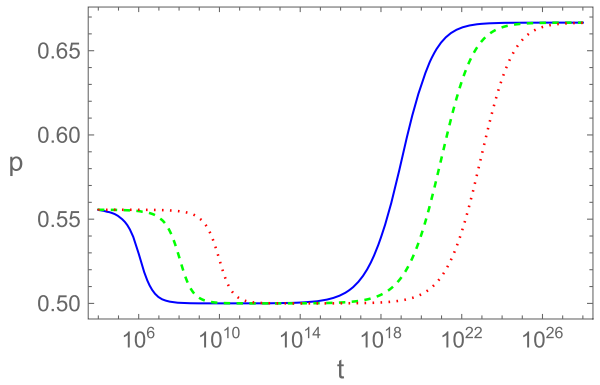

FIG. 10. The profile of $p(t)$ for various values of σ_*. The solid, dashed, and dotted lines correspond to $\sigma_* = 10$, 13, and 16, respectively. The other parameters are chosen as $t_{\rm ref} = 10^4$, $\hat{\beta}_{\rm ref} = 10^{-2}$, and $R_{\rm rad}^{\rm mod} = 10^{-5}$.

Thus, if we define

$$t_{\rm rad} \equiv t(\hat{\beta} = 10), \qquad t_{\rm mod} \equiv t(\hat{\beta}_{\rm mod}), \tag{4.4}$$

the power p changes from $9/5$ to $1/2$ around $t = t_{\rm rad}$, and from $1/2$ to $2/3$ around $t = t_{\rm mod}$. We show a typical profile of the function $p(t)$ in Fig. 9. The parameters are chosen as $\sigma_* = 14$, $\hat{\beta}_{\rm ref} = 10^{-2}$, and $R_{\rm rad}^{\rm mod} = 10^{-5}$.

As we can see from (3.33) and (3.43), the function $p(t)$ depends on the parameters only through $t_{\rm ref}$, $C_{\rm rad}$, $\hat{\beta}_{\rm ref}$, and $R_{\rm rad}^{\rm mod}$. Among them, we choose $t_{\rm ref}$ much smaller than the second term of $t(\hat{\beta})$ in (3.33), and thus its dependence can be neglected. Let us see the dependences on the other three parameters, individually.

$C_{\rm rad}$-dependence

From (3.23), $C_{\rm rad}$ is determined only by σ_* (or $m_{\rm KK}$), and it only affects the overall timescale if $t_{\rm ref}$ is negligible [see (3.33)]. Figure 10 shows the profile of $p(t)$ for different values of σ_*. The solid, dashed, and dotted lines correspond $\sigma_* = 10$, 13 and 16, respectively. As this plot shows, the value of σ_* (i.e., $C_{\rm rad}$) just shift the profile to the time direction without changing its shape.

$\hat{\beta}_{\rm ref}$-dependence

The left plot in Fig. 11 shows the profile of $p(t)$ for various values of $\hat{\beta}_{\rm ref}$. For $\hat{\beta}_{\rm ref} \lesssim 1$, the profile of $p(t)$ is almost independent of $\hat{\beta}_{\rm ref}$, and the initial value of $p(t)$ for $t \ll t_{\rm rad}$ is $9/5$, which is the value of the 6D radiation-dominated universe. For $2 < \hat{\beta}_{\rm ref} < 20$, the value of $p(t)$ at early times ($t \ll t_{\rm rad}$) decreases as $\hat{\beta}_{\rm ref}$ increases. This can be understood from Fig. 8. A larger value of $\hat{\beta}_{\rm ref}$ in this region indicates that the temperature is not high enough for the radiation to feel the compact space S^2 completely, and the 3D space expands less rapidly. For $\hat{\beta}_{\rm ref} > 15$, the radiation no longer feel the compact space, and the expansion rate of the 3D space is almost the same as the 4D radiation-dominated one.

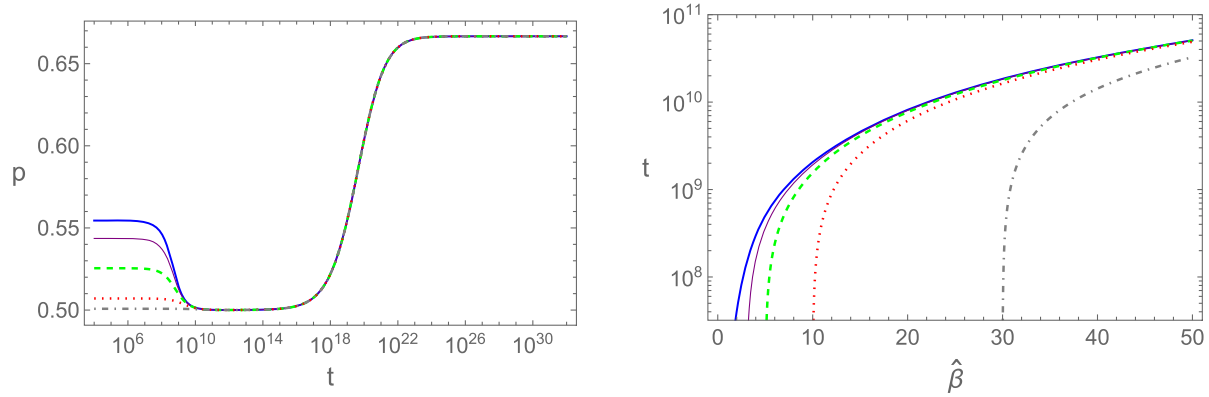

FIG. 11. The profiles of $p(t)$ (left) and $t(\hat{\beta})$ (right). The thick, thin, dashed, dotted, and dot-dashed lines correspond to $\hat{\beta}_{\rm ref} = 1$, 3, 5, 10, and 30, respectively. The other parameters are chosen as $t_{\rm ref} = 10^4$, $\sigma_* = 14$ (i.e., $C_{\rm rad} = 2.97 \times 10^{-16}$), and $R_{\rm rad}^{\rm mod} = 10^{-5}$.

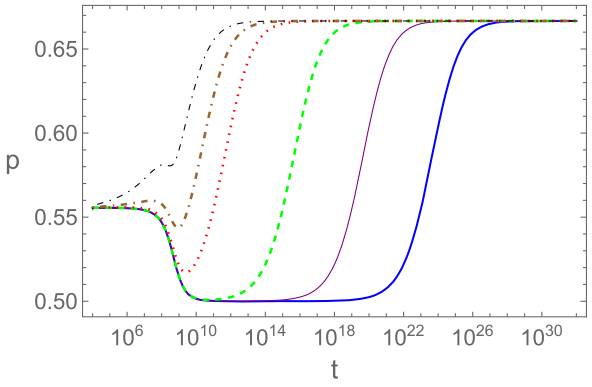

FIG. 12. The profile of $p(t)$. The thick, thin, dashed, dotted, thick dot-dashed, and thin dot-dashed lines correspond to $R_{\rm rad}^{\rm mod} = 10^{-6}$, 10^{-4}, 10^{-2}, 1, 5, and 20, respectively. The other parameters are chosen as $t_{\rm ref} = 10^4$, $\hat{\beta}_{\rm ref} = 0.01$ and $\sigma_* = 14$ (i.e., $C_{\rm rad} = 2.97 \times 10^{-16}$).

The right plot in Fig. 11 shows that a small change of $\hat{\beta}$ corresponds to a large change of t in early times. This explains the plateau for $t \ll t_{\rm rad}$ in the left plot.

$R_{\rm rad}^{\rm mod}$-dependence

Figure 12 shows the $R_{\rm rad}^{\rm mod}$-dependence of $p(t)$. Recall that $R_{\rm rad}^{\rm mod}$ defined in (3.31) parameterizes the ratio of the energy density for the moduli-oscillation to that for the radiation at $t = t_{\rm ref}$. Since the latter energy density decreases faster than the former, the former eventually dominates the total energy density at late times and p will approach to $2/3$. The parameter $R_{\rm rad}^{\rm mod}$ determines $t_{\rm mod}$, at which the moduli-oscillation contribution starts to dominate. For a smaller value of $R_{\rm rad}^{\rm mod}$, it takes more time to dominate the total energy density, and thus $t_{\rm mod}$ becomes larger. When $R_{\rm rad}^{\rm mod} > 1$, on the other hand, the moduli oscillation will dominates the energy density before the universe behaves as the 4D radiation-dominated one.

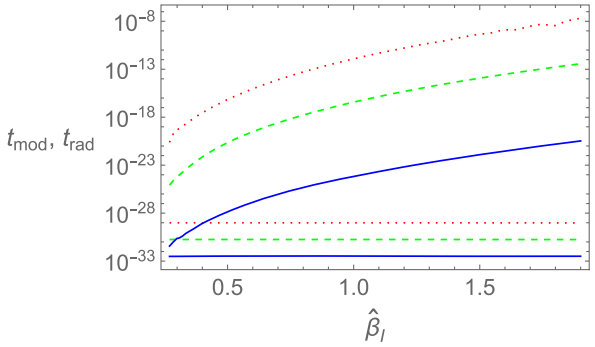

FIG. 13. The transition times $t_{\rm mod}$ and $t_{\rm rad}$ defined in (4.4) as functions of $\hat{\beta}_{\rm I} \equiv m_{\rm KK}\beta_{\rm I}$. The unit of the vertical axis is seconds. The solid, dashed and dotted lines correspond to the case of $\sigma_* = 10$, 13 and 16, respectively. The upper (lower) line represents $t_{\rm mod}$ ($t_{\rm rad}$). The mass parameter m is chosen as $m = 0.01$.

B. Estimation of transition times

So far, we have worked in the 6D Planck unit. For phenomenological discussions, however, it is more convenient to translate the physical quantities in the 4D unit. First, let us restore the dependence of the 6D Planck mass M_6.

$$t \to \frac{t}{M_6}, \qquad \beta \to \frac{\beta}{M_6}, \qquad m_{\rm KK} = e^{-B_*} \to e^{-B_*} M_6. \tag{4.5}$$

The 4D Planck mass M_4 is defined after the extra dimensions are stabilized, and is related to the 6D Planck mass M_6 as

$$M_4 \equiv \sqrt{\mathcal{V}_{2*}} M_6^2 = \sqrt{4\pi} e^{B_*} M_6, \tag{4.6}$$

where $\mathcal{V}_{2*} \equiv 4\pi (e^{B_*} l_6)^2$ ($l_6 \equiv M_6^{-1}$: 6D Planck length) is the volume of the compact space S^2 after the moduli stabilization. Thus, the quantities in (4.5) are expressed as

$$\begin{aligned} t &= \frac{\sqrt{4\pi} e^{B_*}}{M_4} t^{(6)} = 1.46 \times 10^{-18} e^{B_*} t^{(6)}\ {\rm GeV}^{-1} = 8.61 \times 10^{-42} e^{B_*} t^{(6)}\ {\rm sec}, \\ \beta &= \frac{\sqrt{4\pi} e^{B_*}}{M_4} \beta^{(6)} = 1.46 \times 10^{-18} e^{B_*} \beta^{(6)}\ {\rm GeV}^{-1}, \\ m_{\rm KK} &= \frac{M_4}{\sqrt{4\pi} e^{2B_*}} = 6.87 \times 10^{17} e^{-2B_*}\ {\rm GeV}, \end{aligned} \tag{4.7}$$

where $t^{(6)}$ and $\beta^{(6)}$ are the values of the time and the inverse temperature measured by M_6.

Fig. 13 shows the transition times $t_{\rm rad}$ and $t_{\rm mod}$ defined in (4.4) as functions of the initial inverse temperature normalized by the KK mass scale $\hat{\beta}_{\rm I} \equiv m_{\rm KK}\beta_{\rm I}$. The solid, dashed, and dotted lines correspond to the case of $\sigma_* = 10$ ($m_{\rm KK} = 1.2 \times 10^{14}$ GeV), 13 (6.2×10^{12} GeV) and 16 (3.1×10^{11} GeV). From this plot, we see that $t_{\rm mod}$ increases as the initial inverse temperature $\hat{\beta}_{\rm I}$ increases. This can be understood by noting that the induced moduli oscillation

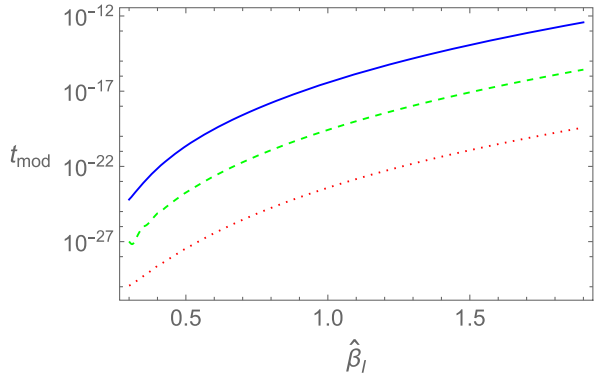

FIG. 14. The transition time $t_{\rm mod}$ defined in (4.4) as functions of $\hat{\beta}_{\rm I} \equiv m_{\rm KK}\beta_{\rm I}$ in the case of $\sigma_* = 12$. The unit of the vertical axis is seconds. The solid, dashed, and dotted lines correspond to the case of $m = 10^{-2}$, 10^{-3}, and 10^{-4}, respectively.

has a larger amplitude for high initial temperature. Namely, for a large value of $\hat{\beta}_{\rm I}$ (i.e., low initial temperature), the pressure $p_2^{\rm rad}$ is small and the induced moduli oscillation has a small amplitude, which leads to a small value of $R_{\rm rad}^{\rm mod}$. As shown in Fig. 12, this means that the moduli oscillation dominates the energy density at later time. In contrast, the transition from the 6D to 4D radiation-dominated eras occurs when the moduli-oscillation energy density is negligible. Therefore, $t_{\rm rad}$ is almost independent of $\hat{\beta}_{\rm I}$, as can be seen from the plot.

Next we see the dependence of the mass parameter m in the moduli potential (2.2). For a smaller value of m, the potential becomes shallower and the moduli can move from the potential minimum (2.4) by the pressure $p_2^{\rm rad}$ more easily. Therefore, the amplitude of the moduli oscillation becomes larger, and the value of $R_{\rm rad}^{\rm mod}$ increases. As a result, we have a smaller value of $t_{\rm mod}$. This behavior can be seen in Fig. 14, which shows the dependence of $t_{\rm mod}$ on m.

From (4.1) and (3.23), the transition time $t_{\rm rad}$ in the M_6 unit is approximated as

$$t_{\rm rad}^{(6)} \simeq t_{\rm ref} + \sqrt{\frac{3}{C_{\rm rad}}}\{\mathcal{G}(10) - \mathcal{G}(\hat{\beta}_{\rm ref})\} \simeq \sqrt{\frac{3}{C_{\rm rad}}}\mathcal{G}(10) = \sqrt{\frac{24\pi^3}{g_{\rm dof}}}e^{3B_*}\mathcal{G}(10). \quad (4.8)$$

Since $\mathcal{G}(10) \simeq 20.6$, $t_{\rm rad}$ in the unit of second is

$$t_{\rm rad} \simeq \sqrt{\frac{24\pi^3}{g_{\rm dof}}}e^{4B_*} \simeq 4.83 \times 10^{-39} \times \frac{e^{4B_*}}{\sqrt{g_{\rm dof}}}\ \text{sec}. \quad (4.9)$$

From (3.33) and (4.4), the transition time $t_{\rm mod}$ in the M_6 unit is approximated as

$$t_{\rm mod}^{(6)} \simeq \sqrt{\frac{3}{2C_{\rm rad}}}\int_{\hat{\beta}_{\rm ref}}^{\hat{\beta}_{\rm mod}} dx \frac{x^2}{v_\beta(x)\sqrt{v_\rho(x)}} \simeq \frac{1}{\pi^2}\sqrt{\frac{6}{C_{\rm rad}}}\hat{\beta}_{\rm mod}^2 \simeq 556\sqrt{\frac{6}{C_{\rm rad}}}(R_{\rm rad}^{\rm mod})^{-2} \simeq 556\sqrt{6}\left(\frac{g_{\rm dof}e^{-6B_*}}{8\pi^3}\right)^{3/2}\tilde{C}_{\rm mod}^{-2} \simeq \frac{0.35 g_{\rm dof}^{3/2}e^{-9B_*}}{\tilde{C}_{\rm mod}^2}, \quad (4.10)$$

where

$$\tilde{C}_{\rm mod} \equiv C_{\rm mod}e^{-3\bar{A}_{\rm ref}+3\mathcal{F}(\hat{\beta}_{\rm ref})}. \quad (4.11)$$

Here we have assumed that $\hat{\beta}_{\rm mod} \gg \hat{\beta}_{\rm ref}$ and used that

$$\frac{x^2}{v_\beta(x)\sqrt{v_\rho(x)}} \simeq \frac{4}{\pi^2}x, \quad (4.12)$$

for $x \gg 1$.

Thus, $t_{\rm mod}$ in the unit of second is

$$t_{\rm mod} = 8.61 \times 10^{-42}e^{B_*}t_{\rm mod}^{(6)}\ \text{sec} \simeq \frac{3.0 \times 10^{-42} g_{\rm dof}^{3/2}e^{-8B_*}}{C_{\rm mod}}e^{3\bar{A}_{\rm ref}-3\mathcal{F}(\hat{\beta}_{\rm ref})}\ \text{sec}. \quad (4.13)$$

Since we are considering the case that $\hat{\beta}_{\rm ref} \ll 1$, we have

$$e^{3\bar{A}_{\rm ref}} \simeq (1+\sqrt{C_A}t_{\rm ref})^{5/3}, \quad \hat{\beta}_{\rm ref} \simeq e^{\frac{3}{5}\bar{A}_{\rm ref}} = (1+\sqrt{C_A}t_{\rm ref})^{1/3}, \quad (4.14)$$

from (3.9). Plugging these and (3.19) into (4.13), we can estimate the value of $t_{\rm mod}$.

C. Moduli decay

The moduli-oscillation-domination era will end by the decay of the moduli. After the lifetime of the moduli $t_{\rm dc}$, the moduli oscillation is converted into the radiation. In this subsection, we will see this effect.

From (3.23), (3.27), (3.31), and (3.32), the radiation energy density is written as

$$\rho^{\rm rad} \simeq C_{\rm rad}\frac{v_\rho(\hat{\beta})}{\hat{\beta}^6} = C_{\rm rad}\frac{e^{-3\mathcal{F}(\hat{\beta})}}{\mathcal{R}(\hat{\beta})} \simeq D_{\rm ref}\frac{e^{-3\bar{A}(\hat{\beta})}}{\hat{\beta}}, \quad (4.15)$$

where

$$D_{\rm ref} \equiv \frac{C_{\rm rad}e^{3\bar{A}_{\rm ref}-3\mathcal{F}(\hat{\beta}_{\rm ref})}}{0.0135}. \quad (4.16)$$

From this, we obtain

$$\dot{\rho}^{\rm rad} \simeq \left(-3\dot{\bar{A}} - \frac{\dot{\hat{\beta}}}{\hat{\beta}}\right)\rho^{\rm rad} \simeq -\{3 + v_\beta(\hat{\beta})\}\dot{\bar{A}}\rho^{\rm rad}, \quad (4.17)$$

where we have used (3.25).

If we introduce the effect of the moduli decay, and (3.20) and (4.17) are modified as

$$\rho^{\rm mod} \simeq C_{\rm mod} e^{-3\bar{A}-\Gamma_{\rm mod} t},$$
$$\dot{\rho}^{\rm rad} \simeq -\{3 + v_\beta(\hat{\beta})\}\dot{\bar{A}}\rho^{\rm rad} + \Gamma_{\rm mod}\rho^{\rm mod}, \quad (4.18)$$

where $\Gamma_{\rm mod} \equiv 1/t_{\rm dc}$ is the total decay rate of the moduli. Recall that

$$t(\hat{\beta}) = t_{\rm ref} + \int_{\hat{\beta}_{\rm ref}}^{\hat{\beta}} \frac{dx}{x v_\beta(x)} \sqrt{\frac{3}{\rho^{\rm rad}(x) + \rho^{\rm mod}(x)}},$$
$$p(\hat{\beta}) = (t - t_{\rm c})\sqrt{\frac{\rho^{\rm rad}(\hat{\beta}) + \rho^{\rm mod}(\hat{\beta})}{3}}, \quad (4.19)$$

where $t_{\rm c}$ is given by (3.39). Now we numerically evaluate p at each time. Denote the value of a quantity q at

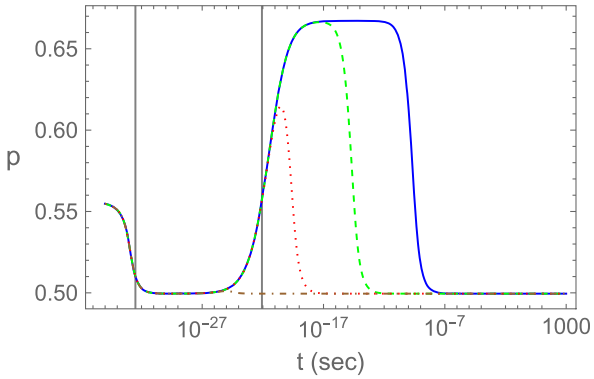

FIG. 15. The profile of $p(t)$ including the moduli decay effect. The solid, dashed, dotted, and dot-dashed lines correspond to the case of $t_{\rm dc} = 10^{-10}$, 10^{-15}, 10^{-20} and 10^{-25} (sec), respectively. The parameters are chosen as $m = 0.01$, $\sigma_* = 10$ and $\beta_{\rm I} = 100$ in the unit of M_6. The vertical lines denote $t_{\rm rad} = 9.5 \times 10^{-30}$ sec (left) and $t_{\rm mod} = 2.3 \times 10^{-21}$ sec (right), respectively.

$$\hat{\beta}_i \equiv \hat{\beta}_{\rm ref} e^{\Delta i}, \quad (i = 0, 1, 2, \ldots) \quad (4.20)$$

where $\Delta \ll 1$ is a small positive constant, as q_i. Then, we have the following recurrence relations.

$$t_{i+1} = t_i + \delta\tau_i,$$
$$\delta\tau_i \equiv \frac{\Delta}{v_\beta(\hat{\beta}_i)}\sqrt{\frac{3}{\rho_i^{\rm rad} + \rho_i^{\rm mod}}},$$
$$\rho_{i+1}^{\rm rad} = \rho_i^{\rm rad} + \delta\tau_i\left[-(3 + v_\beta(\hat{\beta}_i))\sqrt{\frac{\rho_i^{\rm rad} + \rho_i^{\rm mod}}{3}}\rho_i^{\rm rad} + \Gamma_{\rm mod}\rho_i^{\rm mod}\right],$$
$$\rho_{i+1}^{\rm mod} = C_{\rm mod} e^{-3\bar{A}_{i+1} - \Gamma_{\rm mod} t_{i+1}}$$
$$= \rho_i^{\rm mod} \exp\left\{-\frac{\Delta}{v_\beta(\hat{\beta}_i)}\left(3 + \Gamma_{\rm mod}\sqrt{\frac{3}{\rho_i^{\rm rad} + \rho_i^{\rm mod}}}\right)\right\}. \quad (4.21)$$

At the last equality, we have used that

$$\bar{A}_{i+1} = \bar{A}_i + \frac{\Delta}{v_\beta(\hat{\beta}_i)}. \quad (4.22)$$

Using these quantities, the effective power p at $t = t_i$ is calculated as

$$p_i = (t_i - t_{\rm c})\sqrt{\frac{\rho_i^{\rm rad} + \rho_i^{\rm mod}}{3}}. \quad (4.23)$$

Figure 15 shows the effective power p as a function of t in the unit of second. As expected, p rapidly decreases to the radiation-dominated value $1/2$ at $t = t_{\rm dc}$.

V. SUMMARY

We investigated the cosmological expansion of the 3D space in a model with two compact extra dimensions by solving the 6D evolution equations. We assumed that the whole 5D space is filled with the radiation and the moduli have already been stabilized at the initial time. In contrast to the conventional 4D effective theory (4D EFT) analysis, the 6D evolution equations involves the pressure for the compact extra dimensions $p_2^{\rm rad}$. When the temperature of the universe is higher than the compactification scale $m_{\rm KK}$, the pressure $p_2^{\rm rad}$ affects the moduli dynamics.

In our previous work [8], we found that $p_2^{\rm rad}$ pushes out the moduli from the potential minimum, and induces the moduli oscillation. If the moduli lifetime is long enough, the oscillation will eventually dominate the energy density

at late times. In that case, the 3D space expands as $e^A \propto t^{2/3}$. If the temperature of the universe is higher than $m_{\rm KK}$, the radiation feels the whole 5D space, and the 3D space expands as $e^A \propto t^{5/9}$. When the temperature goes down below $m_{\rm KK}$, the radiation ceases to feel the extra dimensions, and the expansion rate slows down as $e^A \propto t^{1/2}$, which is the expansion law of the 4D radiation-dominated universe. In order to pursue these changes of the expansion rate, we define the effective power p in such a way that the 3D scale factor behaves as $e^A \propto t^p$ for each era. The nontrivial expansion of the 3D space is parametrized by two transition times $t_{\rm rad}$ and $t_{\rm mod}$. The effective power p changes from $5/9$ to $1/2$ around $t = t_{\rm rad}$, and from $1/2$ to $2/3$ around $t = t_{\rm rad}$.

In our previous works [7,8], we evaluated the 3D scale factor by numerical computation. However, it is not easy to see how the transition times $t_{\rm rad}$ and $t_{\rm mod}$ depend on the model parameters and the initial temperature in such a numerical approach. Besides, we cannot pursue the whole history of the universe in this method due to the limitation of the computational power. In this paper, we derive analytic expressions for the 3D scale factor, the inverse temperature and the background moduli values by solving the 6D evolution equations under appropriate approximations, and provide analytic expressions for the transition times as functions of the model parameters m, σ_* and the initial (inverse) temperature $\beta_{\rm I}$. The expressions we obtained enable us to pursue the cosmological evolution until much later times.

The first transition time $t_{\rm rad}$ is determined solely by σ_* (or $m_{\rm KK}$), and is almost independent of the initial temperature. The second transition time $t_{\rm mod}$, on the other hand, depends on both the moduli potential scale m and the temperature. This is because $t_{\rm mod}$ is determined by the oscillation amplitude induced by $p_2^{\rm rad}$. The amplitude becomes larger for a shallower potential (i.e., a smaller value of m or a larger value of σ_*) or for higher initial temperature (i.e., a smaller value of $\beta_{\rm I}$), and then the moduli oscillation dominates the energy density earlier (a smaller value of $t_{\rm mod}$).

As shown in Ref. [7], the modulus B continues to increase for $\sigma_* \gtrsim 16$, and the observed 4D universe cannot be obtained. Therefore, there is an upper bound for the stabilized value of the S^2 radius in our model.

In our works, we have fixed the moduli by introducing the dilaton mass term by hand. It should be noted that there are other types of moduli stabilization mechanisms. For example, it is shown that the moduli can be stabilized by introducing 3-branes with the dilaton couplings in Refs. [22–26]. This corresponds to a 6D extension of the Goldberger-Wise mechanism [27] in the Randall-Sundrum setup [28]. It is intriguing to study whether the properties we found here will change in such models. From the viewpoint of the 4D EFT, both stabilization mechanisms just generate the moduli potential and thus it seems that they lead to similar results. However, it is nontrivial whether this is the case when the 4D EFT is not valid.

For more realistic discussions, we need to extend our setup by including the inflaton sector. Our initial conditions in (2.11) with the radiation-domination assumption should be realized by the reheating process after the inflation. In such setups, the effective power p will enter the expression of the e-folding number for the 3D scale factor.

We will discuss the above issues in separate papers.

APPENDIX A: THERMODYNAMIC QUANTITIES

The dispersion relation of a 6D relativistic or massless particle is

$$k^M k_M = -k_0^2 + e^{-2A}\vec{k}^2 + e^{-2B}k_\theta^2 + \frac{1}{e^{2B}\sin^2\theta}k_\phi^2 = 0. \tag{A1}$$

Thus the energy of the particle with the 3D momentum $\vec{k} = (k_1, k_2, k_3)$ and the angular momentum l on S^2 is given by

$$\mathcal{E}_{k,l} = k_0 = \sqrt{e^{-2A}k^2 + e^{-2B}l(l+1)}, \tag{A2}$$

where $k \equiv \sqrt{\vec{k}^2}$. Since each one-particle state is specified by $\vec{k}$, l and the "magnetic quantum number" $m = -l, \ldots, l$, we have $(2l+1)$ degenerate energy eigenstates for each $\vec{k}$ and l. Hence the grand potential is expressed as

$$\begin{aligned} J(\beta, \mu, \mathcal{V}_3, \mathcal{V}_2) &= \pm \sum_{l=0}^{\infty} \frac{g_{\rm dof}(2l+1)}{2\pi^2\beta} \int_0^\infty dk k^2 \ln(1 \mp e^{-\beta(\mathcal{E}_{k,l}-\mu)}) \\ &= \mp \frac{g_{\rm dof}\mathcal{V}_3}{\pi^2\beta^4} \mathrm{Li}_4(\pm e^{\beta\mu}) \pm \sum_{l=1}^{\infty} \frac{g_{\rm dof}(2l+1)\mathcal{V}_3}{2\pi^2\beta^4} \int_0^\infty dq q^2 \ln(1 \mp e^{-\sqrt{q^2+c_l^2}+\beta\mu}), \end{aligned} \tag{A3}$$

where $g_{\rm dof}$ denotes the degrees of freedom for the 6D relativistic particles, β is the inverse temperature, μ is the chemical potential, and $\mathcal{V}_3 \equiv e^{3A}$ and $\mathcal{V}_2 \equiv 4\pi e^{2B}$ are the comoving volume for the 3D space and the physical volume of S^2, respectively. The upper (lower) signs correspond to the case of bosons (fermions). At the second equality, we have rescaled the integration variable and the KK masses as

$$q \equiv e^{-A}\beta k, \qquad c_l \equiv \beta\sqrt{\frac{4\pi l(l+1)}{\mathcal{V}_2}} = e^{-B}\beta\sqrt{l(l+1)}. \tag{A4}$$

The function $\mathrm{Li}_4(z)$ in the second line of (A3) is the polylogarithmic function. In the following, we consider a situation in which $e^{-c_l+\beta\mu} \ll 1$ for $l \geq 1$. Then the grand potential can be approximated as

$$J(\beta,\mu,\mathcal{V}_3,\mathcal{V}_2) \simeq -\frac{g_{\mathrm{dof}}\mathcal{V}_3}{2\pi^2\beta^4}\left\{\pm 2\mathrm{Li}(\pm e^{\beta\mu}) + e^{\beta\mu}Q_1\left(\beta\sqrt{\frac{4\pi}{\mathcal{V}_2}}\right)\right\}, \tag{A5}$$

where

$$Q_1(x) \equiv \sum_{l=1}^{\infty} x^2 l(l+1)(2l+1)K_2(x\sqrt{l(l+1)}). \tag{A6}$$

Here $K_2(z)$ is the modified Bessel function of the second kind.

From (A3), various thermodynamic quantities are calculated as follows.

Radiation energy density

$$\rho^{\mathrm{rad}} = \frac{1}{\mathcal{V}_3\mathcal{V}_2}\left(\partial_\beta - \frac{\mu}{\beta}\partial_\mu\right)(\beta J) \simeq \frac{g_{\mathrm{dof}}}{2\pi^2\beta^4\mathcal{V}_2}\{\pm 6\mathrm{Li}_4(\pm e^{\beta\mu}) + e^{\beta\mu}(3Q_1+Q_2)\}, \tag{A7}$$

where

$$Q_2(x) \equiv -xQ_1'(x) = \sum_{l=1}^{\infty} x^3 l^{3/2}(l+1)^{3/2}(2l+1) \times K_1(x\sqrt{l(l+1)}). \tag{A8}$$

3D pressure

$$p_3^{\mathrm{rad}} = -\frac{1}{\mathcal{V}_2}\frac{\partial J}{\partial \mathcal{V}_3} \simeq \frac{g_{\mathrm{dof}}}{2\pi^2\beta^4\mathcal{V}_2}\{\pm 2\mathrm{Li}_4(\pm e^{\beta\mu}) + e^{\beta\mu}Q_1\}. \tag{A9}$$

2D pressure

$$p_2^{\mathrm{rad}} = -\frac{1}{\mathcal{V}_3}\frac{\partial J}{\partial \mathcal{V}_2} \simeq \frac{g_{\mathrm{dof}}e^{\beta\mu}}{4\pi^2\beta^4\mathcal{V}_2}Q_2. \tag{A10}$$

The arguments of the functions Q_1 and Q_2 are understood as $\beta\sqrt{4\pi/\mathcal{V}_2} = e^{-B}\beta$.

We should note that

$$\rho^{\mathrm{rad}} = 3p_3^{\mathrm{rad}} + 2p_2^{\mathrm{rad}}. \tag{A11}$$

In this paper, we assume that $\beta\mu \ll 1$ and neglect the chemical potential μ. Note that

$$\mathrm{Li}_4(1) = \zeta(4) = \frac{\pi^4}{90}, \qquad \mathrm{Li}_4(-1) = -\frac{7}{8}\zeta(4). \tag{A12}$$

If we have the same degrees of freedom for bosons and fermions, the total energy density and pressures are expressed as

$$\rho^{\mathrm{rad}} \simeq \frac{g_{\mathrm{dof}}}{2\pi^2\beta^4\mathcal{V}_2}\left\{\frac{\pi^4}{16} + 3Q_1(e^{-B}\beta) + Q_2(e^{-B}\beta)\right\},$$
$$p_3^{\mathrm{rad}} \simeq \frac{g_{\mathrm{dof}}}{2\pi^2\beta^4\mathcal{V}_2}\left\{\frac{\pi^4}{48} + Q_1(e^{-B}\beta)\right\},$$
$$p_2^{\mathrm{rad}} \simeq \frac{g_{\mathrm{dof}}}{4\pi^2\mathcal{V}_2}Q_2(e^{-B}\beta), \tag{A13}$$

where g_{dof} is the total degrees of freedom for the radiation.

APPENDIX B: CONSERVATION LAW

Including the radiation contribution, the energy-momentum conservation law is

$$\nabla_M T^M_N \equiv \partial_M T^M_N + \Gamma^M_{ML}T^L_N - \Gamma^L_{MN}T^M_L = 0, \tag{B1}$$

where

$$T^t_t = \frac{1}{2}\dot{\sigma}^2 + \frac{e^\sigma}{8b^4} + V(\sigma) + \rho^{\mathrm{rad}} \equiv \rho^{\mathrm{tot}},$$
$$T^i_j = \delta^i_j\left\{-\frac{1}{2}\dot{\sigma}^2 + \frac{e^\sigma}{8b^4} + V(\sigma) - p_3^{\mathrm{rad}}\right\} \equiv -\delta^i_j p_3^{\mathrm{tot}},$$
$$T^4_4 = T^5_5 = -\frac{1}{2}\dot{\sigma}^2 - \frac{e^\sigma}{8b^4} + V(\sigma) - p_2^{\mathrm{rad}} \equiv -p_2^{\mathrm{tot}}. \tag{B2}$$

From (B1) with $N = t$, we have

$$\dot{\rho}^{\mathrm{tot}} + 3\dot{A}(\rho^{\mathrm{tot}} + p_3^{\mathrm{tot}}) + 2\dot{B}(\rho^{\mathrm{tot}} + p_2^{\mathrm{tot}}) = 0, \tag{B3}$$

where the dot denotes the time derivative. The other components hold trivially. By using the dilaton field equation, the conservation law (B3) is reduced to

$$\dot{\rho}^{\mathrm{rad}} + (3\dot{A} + 2\dot{B})\rho^{\mathrm{rad}} + 3\dot{A}p_3^{\mathrm{rad}} + 2\dot{B}p_2^{\mathrm{rad}} = 0. \tag{B4}$$

Plugging (A13) into this, we obtain

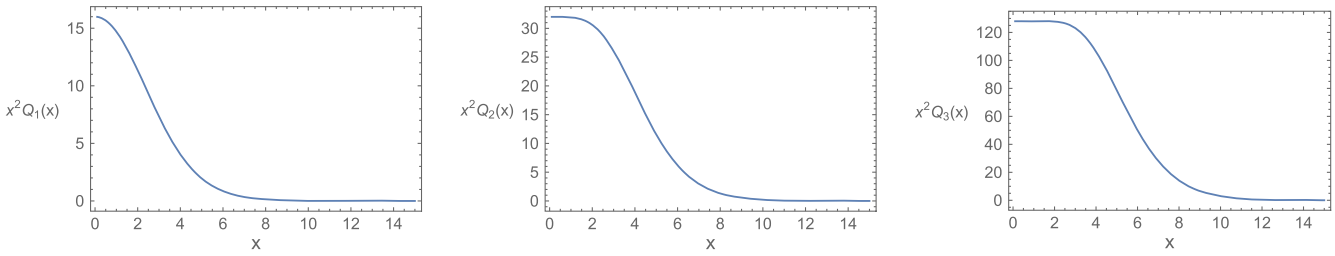

FIG. 16. The profile of $x^2Q_1(x)$, $x^2Q_2(x)$, and $x^2Q_3(x)$.

$$\frac{\dot\beta}{\beta}\left(\frac{\pi^4}{4}+12Q_1+5Q_2+Q_3\right) = 3\dot A\left(\frac{\pi^4}{12}+4Q_1+Q_2\right)+\dot B(2Q_2+Q_3), \tag{B5}$$

where

$$Q_3(x) \equiv 2Q_2(x)-xQ_2'(x) = \sum_{l=1}^{\infty} x^4 l^2(l+1)^2(2l+1)K_0(x\sqrt{l(l+1)}). \tag{B6}$$

The arguments of $Q_{1,2,3}$ are understood as $e^{-B}\beta$.

Figure 16 shows the profiles of $Q_{1,2,3}(x)$. For $x \ll 1$, they are approximated as

$$Q_1(x) \simeq \frac{16}{x^2}, \qquad Q_2(x) \simeq \frac{32}{x^2}, \qquad Q_3(x) \simeq \frac{128}{x^2}. \tag{B7}$$

APPENDIX C: INDUCED OSCILLATION SOLUTION

Here we provide a solution of the following equation for a real function $\varphi(t)$.

$$\ddot\varphi = -\lambda\varphi + \frac{\alpha}{(1+\sqrt{C}t)^q}, \tag{C1}$$

where $\lambda > 0$, $C > 0$, α and q are real constants. The solution is expressed as

$$\varphi(t) = c_1\cos(\sqrt{\lambda}t)+c_2\sin(\sqrt{\lambda}t) -\frac{\alpha}{\lambda}\left(\frac{\lambda}{C}\right)^{\frac{q}{2}}\mathcal{S}\left(\sqrt{\frac{\lambda}{C}}(1+\sqrt{C}t)\right), \tag{C2}$$

where c_1 and c_2 are integration constants, and

$$\mathcal{S}(x) \equiv \mathrm{Im}\{e^{(q-1)\frac{\pi}{2}i}\mathcal{E}_q(ix)\},$$
$$\mathcal{E}_q(x) \equiv e^z\frac{\mathrm{E}_q(z)}{z^{q-1}} = e^z\Gamma(1-q,z). \tag{C3}$$

The function $\mathrm{E}_q(z) \equiv \int_1^\infty dw e^{-zw}/w^q$ is the (generalized) exponential integral, and $\Gamma(s,z)$ is the upper incomplete gamma function. The derivatives of the real function $\mathcal{S}(x)$ are

$$\mathcal{S}'(x) = \mathrm{Re}\{e^{(q-1)\frac{\pi}{2}i}\mathcal{E}_q'(ix)\} = \mathrm{Re}\{e^{(q-1)\frac{\pi}{2}i}\mathcal{E}_q(ix)\},$$
$$\mathcal{S}''(x) = -\mathrm{Im}\{e^{(q-1)\frac{\pi}{2}i}\mathcal{E}_q'(ix)\} = -\frac{1}{x^q}-\mathcal{S}(x). \tag{C4}$$

We have used that

$$\mathcal{E}_q'(z) = \frac{-1+e^z z\mathrm{E}_q(z)}{z^q} = -\frac{1}{z^q}+e^z\Gamma(1-q,z) = -\frac{1}{z^q}+\mathcal{E}_q(z). \tag{C5}$$

When the initial condition is that $\varphi(0) = \dot\varphi(0) = 0$, the solution becomes

$$\varphi(t) = -\frac{\alpha}{\lambda}\left(\frac{\lambda}{C}\right)^{\frac{q}{2}}\left\{\mathcal{S}\left(\sqrt{\frac{\lambda}{C}}(1+\sqrt{C}t)\right) -\mathcal{S}\left(\sqrt{\frac{\lambda}{C}}\right)\cos(\sqrt{\lambda}t)-\mathcal{S}'\left(\sqrt{\frac{\lambda}{C}}\right)\sin(\sqrt{\lambda}t)\right\} = -\frac{\alpha}{\lambda}\left(\frac{\lambda}{C}\right)^{\frac{q}{2}}\mathrm{Im}\{e^{(q-1)\frac{\pi}{2}i}\mathcal{U}_q(t;\lambda,C)\}, \tag{C6}$$

where

$$\mathcal{U}_q(t;\lambda,C) \equiv \mathcal{E}_q\left(i\sqrt{\frac{\lambda}{C}}(1+\sqrt{C}t)\right) - \mathcal{E}_q\left(i\sqrt{\frac{\lambda}{C}}\right)e^{i\sqrt{\lambda}t}$$
$$= e^{i\sqrt{\frac{\lambda}{C}}(1+\sqrt{C}t)}\left\{\Gamma\left(1-q, i\sqrt{\frac{\lambda}{C}}(1+\sqrt{C}t)\right) - \Gamma\left(1-q, i\sqrt{\frac{\lambda}{C}}\right)\right\}. \tag{C7}$$

The derivative of (C6) is expressed as

$$\dot{\varphi} = -\alpha\left(\frac{\lambda}{C}\right)^{\frac{q}{2}}\mathrm{Re}\{e^{(q-1)\frac{\pi}{2}i}\mathcal{U}_q(t;\lambda,C)\}. \tag{C8}$$

[1] Nima Arkani-Hamed, Savas Dimopoulos, and G. R. Dvali, The hierarchy problem and new dimensions at a millimeter, Phys. Lett. B **429**, 263 (1998).

[2] Nima Arkani-Hamed, Savas Dimopoulos, and G. R. Dvali, Phenomenology, astrophysics and cosmology of theories with submillimeter dimensions and TeV scale quantum gravity, Phys. Rev. D **59**, 086004 (1999).

[3] Ignatios Antoniadis, Nima Arkani-Hamed, Savas Dimopoulos, and G. R. Dvali, New dimensions at a millimeter to a Fermi and superstrings at a TeV, Phys. Lett. B **436**, 257 (1998).

[4] Y. Aghababaie, C. P. Burgess, S. L. Parameswaran, and F. Quevedo, Towards a naturally small cosmological constant from branes in 6-D supergravity, Nucl. Phys. **B680**, 389 (2004).

[5] Dieter Lüst, Eran Palti, and Cumrun Vafa, AdS and the swampland, Phys. Lett. B **797**, 134867 (2019).

[6] Miguel Montero, Cumrun Vafa, and Irene Valenzuela, The dark dimension and the swampland, J. High Energy Phys. 02 (2023) 022.

[7] Hajime Otsuka and Yutaka Sakamura, Spacetime evolution during moduli stabilization in radiation dominated era beyond 4D effective theory, J. High Energy Phys. 08 (2022) 120.

[8] Hajime Otsuka and Yutaka Sakamura, Full higher-dimensional analysis of moduli oscillation and radiation in expanding universe, J. High Energy Phys. 05 (2023) 231.

[9] H. Nishino and E. Sezgin, Matter and gauge couplings of $N = 2$ supergravity in six- dimensions, Phys. Lett. **144B**, 187 (1984).

[10] C. P. Burgess, Supersymmetric large extra dimensions and the cosmological constant: An Update, Ann. Phys. (Amsterdam) **313**, 283 (2004).

[11] C. P. Burgess, F. Quevedo, G. Tasinato, and I. Zavala, General axisymmetric solutions and self-tuning in 6D chiral gauged supergravity, J. High Energy Phys. 11 (2004) 069.

[12] Jaume Garriga and Massimo Porrati, Football shaped extra dimensions and the absence of self-tuning, J. High Energy Phys. 08 (2004) 028.

[13] Luis A. Anchordoqui, Ignatios Antoniadis, Dieter Lüst, and Jorge F. Soriano, Dark energy, Ricci-nonflat spaces, and the swampland, Phys. Lett. B **816**, 136199 (2021).

[14] Mirjam Cvetic, G. W. Gibbons, and C. N. Pope, A string and M theory origin for the Salam-Sezgin model, Nucl. Phys. **B677**, 164 (2004).

[15] Takeo Moroi and Tomo Takahashi, Effects of cosmological moduli fields on cosmic microwave background, Phys. Lett. B **522**, 215 (2001); **539**, 303(E) (2002).

[16] S. Randjbar-Daemi, Abdus Salam, E. Sezgin, and J. A. Strathdee, An anomaly free model in six-dimensions, Phys. Lett. **151B**, 351 (1985).

[17] G. W. Gibbons, Rahmi Gueven, and C. N. Pope, 3-branes and uniqueness of the Salam- Sezgin vacuum, Phys. Lett. B **595**, 498 (2004).

[18] Y. Aghababaie, C. P. Burgess, James M. Cline, H. Firouzjahi, S. L. Parameswaran, F. Quevedo, G. Tasinato, and I. Zavala, Warped brane worlds in six-dimensional supergravity, J. High Energy Phys. 09 (2003) 037.

[19] Hyun Min Lee and Christoph Ludeling, The general warped solution with conical branes in six-dimensional supergravity, J. High Energy Phys. 01 (2006) 062.

[20] Michael B. Green, John H. Schwarz, and Peter C. West, Anomaly free chiral theories in six-dimensions, Nucl. Phys. **B254**, 327 (1985).

[21] Vijay Kumar, David R. Morrison, and Washington Taylor, Global aspects of the space of 6D $N = 1$ supergravities, J. High Energy Phys. 11 (2010) 118.

[22] A. J. Tolley, C. P. Burgess, C. de Rham, and D. Hoover, Scaling solutions to 6D gauged chiral supergravity, New J. Phys. **8**, 324 (2006).

[23] Leo van Nierop and C. P. Burgess, Sculpting the extra dimensions: Inflation from codimension-2 brane back-reaction, J. Cosmol. Astropart. Phys. 04 (2012) 037.

[24] C. P. Burgess and L. van Nierop, Large dimensions and small curvatures from supersymmetric brane back-reaction, J. High Energy Phys. 04 (2011) 078.

[25] C. P. Burgess, Ross Diener, and M. Williams, Self-tuning at large (distances): 4D description of runaway dilaton capture, J. High Energy Phys. 10 (2015) 177.

[26] C. P. Burgess, Jared J. H. Enns, Peter Hayman, and Subodh P. Patil, Goldilocks models of higher-dimensional inflation (including modulus stabilization), J. Cosmol. Astropart. Phys. 08 (2016) 045.

[27] Walter D. Goldberger and Mark B. Wise, Modulus stabilization with bulk fields, Phys. Rev. Lett. **83**, 4922 (1999).

[28] Lisa Randall and Raman Sundrum, A large mass hierarchy from a small extra dimension, Phys. Rev. Lett. **83**, 3370 (1999).